PCCP

COMMUNICATION

View Article Online
View Journal

Cite this: DOI: 10.1039/c9cp00448c

Received 24th January 2019,
Accepted 12th March 2019

DOI: 10.1039/c9cp00448c

rsc.li/pccp

Structural and magnetic studies of $KOsO_4$, a $5d^1$ quantum magnet oxide†

Sean Injac,[a] Alexander K. L. Yuen,[a] Maxim Avdeev,[ab] Fabio Orlandi[c] and Brendan J. Kennedy*[a]

The quantum magnet $KOsO_4$ has been characterized by a combination of X-ray and neutron diffraction techniques. The tetrahedrally coordinated Os^{7+} $5d^1$ S = 1/2 cations were determined to order antiferromagnetically along the c axis below 35 K. A miniscule ordered magnetic moment of 0.46(18) μ_B was determined per Os^{7+} cation.

Oxides containing 5d transition metals are currently attracting considerable attention due to their interesting, and often unusual, magnetic properties such as the ferromagnetic insulator Ba_2NiOsO_6 and the superconducting oxide KOs_2O_6.[1] These magnetic behaviours are generally attributed to the diffuse nature of the 5d orbitals, which can give rise to itinerant, rather than localized, electron behaviour and pronounced spin–orbit coupling effects. Spin–orbit coupling often results in a significant decrease of the observed magnetic moment, as illustrated in numerous Re, Os and Ir containing compounds.[2–7] Further examples include the $5d^1$ oxides Ba_2NaOsO_6, Ba_2LiOsO_6, and Ba_2MReO_6 (M = Mg, Zn) which show strongly quenched antiferromagnetic and ferromagnetic ground states.[8–12] The majority of studies of 5d oxides reported to date describe structures based on corner sharing octahedral motifs such as perovskites and pyrochlores where superexchange plays a significant role in the observed magnetic ground state. This is in contrast to the ABO_4 scheelite structure, in which the smaller B cation is tetrahedrally coordinated by oxygen anions. The ionic nature of the larger A cation drives a close-packed structure of these and the BO_4 anion moieties. The isolated nature of the BO_4 tetrahedra removes oxygen-mediated superexchange interactions. A recent study of isostructural $KRuO_4$, (Ru^{7+}, $4d^1$, S = 1/2) has shown this to be antiferromagnetic T_N = 22.4 K, with a small ordered magnetic moment of 0.57 μ_B.[13] The AFM ordering occurs along the c axis and is consistent with a low dimensional spin model. The strong covalent nature of the Ru–O bond drives delocalisation of the $4d^1$ electron about the RuO_4 tetrahedra, further suppressing magnetic ordering.

A small number of mixed potassium osmate systems have been reported, the primary examples being the superconducting pyrochlore KOs_2O_6; with a superconducting critical temperature of 9.6 K, the diamagnetic Os^{8+} compound K_2OsO_5, in which the Os cations occupy a trigonal bipyramidal OsO_5 coordination environment, and the oxidizing agent $KOsO_4$, first reported by Levason in 1985.[14–16] A recent DFT study suggests that $KOsO_4$ will have Mott-insulating antiferromagnetic ground state.[17]

In this study $KOsO_4$ was synthesized and its structure and magnetic properties investigated. $KOsO_4$ is isoelectric and isostructural to $KRuO_4$, and changes in magnetic character can be attributed to the more diffuse nature of the 5d orbitals, increased spin–orbit coupling, and electron delocalization. $KOsO_4$ allows for investigation of the magnetic character of a single 5d electron magnet, in which magnetic interactions are primarily mediated by spin–spin interactions between electronically isolated OsO_4 tetrahedra. This unique case allows for further fundamental insight into the nature of magnetism in the relatively less studied 5d metal systems.

Polycrystalline $KOsO_4$ was prepared using standard Schlenk techniques using a modification of the method of Levason.[14] 1.0 g of osmium tetroxide (Alfa Aesar, 99.8%) was dissolved in 20 mL dried acetone, and this solution was transferred *via* cannula to a solution of 0.98 g potassium iodide (AJAX Finechem, >99%) (1.5 molar equivalents of K : Os) in dried acetone. The solution was stirred for 1 hour at ambient temperature, under nitrogen flow. The solution volume was then reduced under a stream of nitrogen and the resulting $KOsO_4$ precipitate was isolated by vacuum filtration, washed with acetone, and air dried. The sample was stored under dry nitrogen. While the compound is both air and moisture stable, exposure to oxidizing conditions liberates OsO_4. Care must be taken when working with OsO_4, which readily sublimes at room temperature. All manipulations

[a] School of Chemistry, The University of Sydney, Sydney, NSW 2006, Australia. E-mail: Brendan.Kennedy@Sydney.edu.au
[b] Australian Nuclear Science and Technology Organisation, Lucas Heights, NSW 2234, Australia
[c] ISIS Neutron Pulsed Facility, Science and Technology Facilities Council, Rutherford Appleton Laboratory, Oxford OX11 0QX, UK

† Electronic supplementary information (ESI) available. See DOI: 10.1039/c9cp00448c

were performed in a fume cupboard using Schlenk techniques and appropriate personal protective equipment.

X-ray diffraction measurements were undertaken at the Powder Diffraction beamline, BL-10, at the Australian Synchrotron.[18] The sample was sealed in a 0.2 mm diameter quartz capillary which was rotated within the beam during data collection. Data were collected at 21 keV (λ = 0.58910 Å) as determined by calibration against a LaB_6 standard. Datasets were collected at temperatures between 90 K and 740 K in 10° steps using an Oxford cryostream or hot air blower. Structural refinements were undertaken using the program FullProf.[19]

Neutron powder diffraction data were collected at the high resolution diffractometer, ECHIDNA at ANSTO's OPAL reactor[20] and at the WISH diffractometer at the ISIS spallation source.[21] The former measurements were conducted at room temperature and 1.5 K using neutrons of wavelength 1.6227 Å and 2.4395 Å respectively. Data on WISH were measured between 0.43 Å $\leq d \leq$ 48 Å in 5 detectors banks with average 2θ of 152.8, 121.6, 90.0, 58.3 and 27.0 degrees, each covering 32 degrees of the scattering plane. Diffraction data were collected at 1.5 K, 100 K and between temperatures of 10 K and 70 K in 10° steps.

Temperature dependent DC magnetic susceptibility and heat capacity data were collected 2 K and 300 K using a Quantum Design PPMS. Magnetic susceptibility data were collected from a powder sample, under zero field cooled (ZFC) and field cooled (FC) conditions with an external field of 0.1 T. The ZFC data were collected on heating from 2 K, and ZFC data were collected upon cooling from 300 K. Isothermal magnetization measurements were undertaken at 2 K, with an applied external magnetic field between -9×10^5 Oe and 9×10^5 Oe. Heat capacity measurements employed the relaxation technique using a pellet sample.

X-ray absorption spectroscopy measurements at the Os L_3 edge were conducted at the XAS beamline of the Australian Synchrotron.[22] Measurements were performed at room temperature in transmission mode using argon-filled ionisation chambers. The beam intensity (I_0) was monitored by an ionisation chamber located upstream from the sample. XANES spectra were collected by a second ionisation chamber after the sample. A third ionisation chamber was placed downstream to simultaneously measure a reference spectrum of Os powder. Energy steps as small as 0.25 eV were employed near the absorption edge with a counting time of 2 s per step. The energy scale of the monochromator was calibrated using the L_3-edge of a Pt foil at 11562.7 eV and the Os reference spectra were used to align scans from different samples. Data analysis was carried out using the software package ATHENA.[23]

At room temperature $KOsO_4$ adopts a tetragonal scheelite type structure in space group $I4_1/a$, with a = 5.67586(1) c = 12.71914(1) Å and the structure was refined using the Rietveld method against a combined synchrotron and neutron powder diffraction dataset. Refinement profiles are shown in Fig. 1. The refined Os–O distance of 1.732(2) Å is comparable to that reported for OsO_4 (1.70 Å) and to that reported for isostructural $KRuO_4$ (1.742(4) Å).[24] Details are available in the ESI.†

The structure exists between 1.5 K and 500 K, heating beyond this temperature resulted in decomposition of the sample. A slight anomaly is observed in the thermal expansion of the

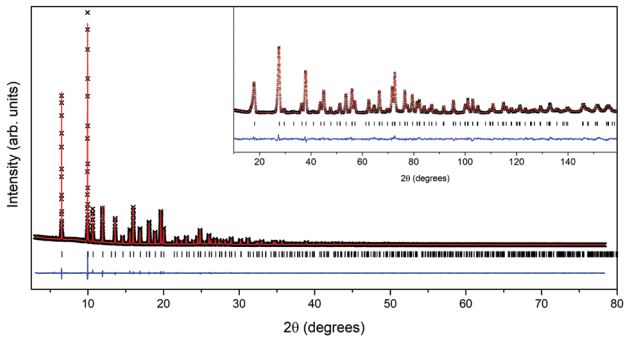

Fig. 1 Rietveld refinement profiles of SXRD data (λ = 0.58910 Å, χ^2 = 2.96) and NPD data, shown in inset (λ = 1.6227 Å, χ^2 = 1.72) for $KOsO_4$ collected at room temperature. Observed data are indicated by black crosses, the calculated profile is shown in red and difference plot is shown in blue. Black vertical marks indicate the positions of the space group allowed *hkl* reflections.

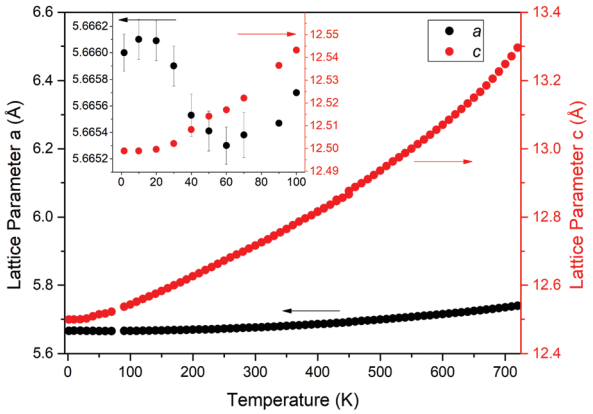

Fig. 2 Evolution of the refined values of lattice parameters *a* (black dots) and *c* (red dots) with temperature between 1.5 K and 720 K. The data for $T \geq$ 90 K were refined against SXRD data while those for $T \leq$ 70 K were obtained from WISH NPD data. The inset shows data for $0 < T \leq 100$ K. Where not apparent the error bars are smaller than the symbols.

lattice parameters, Fig. 2, near 35 K, where the *a* lattice parameter was observed to increase while the *c* lattice parameter decreases. This is a consequence of magnetic ordering, described in more detail below. No significant changes in the oxygen positional parameters, and hence Os–O bond lengths were observed until the onset of the thermally induced decomposition at approximately 740 K. The Os L_3-XANES spectrum of $KOsO_4$, corresponding to the $2p_{3/2} \rightarrow 5d_{3/2,5/2}$ dipole transitions, was measured at room temperature and compared to Os^{4+}, Os^{5+} and Os^{6+} standards. These data are shown in the ESI.† There is a slight shift in the observed absorbance edge as well as the distinct change in near edge structure from those observed for the Os standards in which Os is in an octahedral coordination environment. The Os L_3-edge XANES spectra consist of two components corresponding to the t_2 and e orbitals due to crystal field splitting of the Os (5d) states by the tetrahedral field.[25]

Temperature dependent DC magnetic susceptibility data, collected between 2 and 300 K, are shown in Fig. 3. A broad feature with a maximum at approximately 60 K is observed,

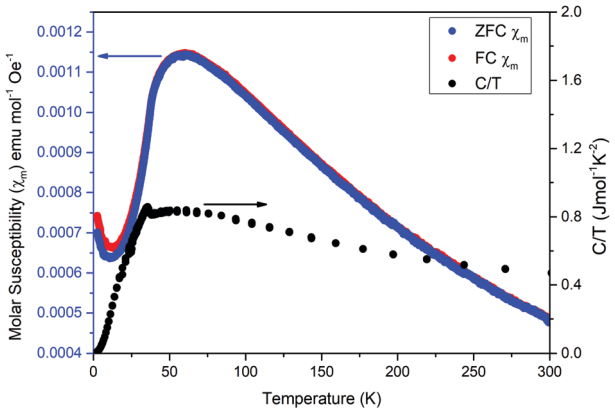

Fig. 3 Temperature dependent magnetic susceptibility data collected for $2 \leq T \leq 300$ K. Data collected under zero field cooled conditions are shown in blue and data collected under field cooled conditions are shown in red (values on left axis). Heat capacity data are shown in black (values on right axis).

consistent with antiferromagnetic ordering. A slight divergence of the ZFC and FC curves is observed below this temperature. An effective magnetic moment 1.42 μ_B was determined by fitting the paramagnetic region (taken to be $T > 100$ K) to the Curie Weiss law with $\Theta = -43.8$ K. The temperature dependence of the magnetic moment, illustrated in Fig. S5 (ESI†), is similar to that seen by Mogare *et al.*[15] for weakly antiferromagnetic K_2OsO_5. This value is in excellent agreement with that reported previously (1.4(1) μ_B) and is lower than that reported for $KRuO_4$, (near 1.73 μ_B).[13,14] The larger reduction in the paramagnetic moment in $KOsO_4$ from the spin only value of 1.73 μ_B is consistent with increased spin–orbit coupling of the 5d verses 4d electrons. Isothermal magnetization measurements, collected at 2 K, show no spontaneous magnetization: the observed magnetic moment remains essentially linear to 9×10^4 Oe (data shown in ESI†). The observations from magnetic susceptibility and isothermal magnetization measurements indicate an antiferromagnetic spin arrangement as the magnetic ground state. Heat capacity data shows, in Fig. 3, a peak at 35 K consistent with AFM ordering. The observed lambda-type thermal anomaly (Fig. S5, ESI†) is associated with magnetic ordering. The heat capacity contains magnetic, lattice and crystal field (CF) contributions.[26] Generally the CF contribution for transition metals is sufficiently small so that it can be neglected. The lattice contribution to the heat capacity was estimated using a 5th order polynomial and the magnetic contribution to the entropy was determined to be 1.39 J K^{-1} mol^{-1} by subtraction of the lattice contributions and integration of the C/T curve between 25 K and 40 K. This is less than the theoretical $R\ln(2S + 1)$ value of 5.76 J K^{-1} mol^{-1} suggesting there may be some diffuse magnetic ordering. This is consistent with the broad feature observed in the magnetic susceptibility data. The neutron powder diffraction data collected at the WISH diffractometer revealed the presence of a single magnetic reflection at $d = 4.0$ Å for all datasets collected below 40 K; no other significant intensity changes were observed. This peak was indexed as 110 to a $k = (0,0,0)$ magnetic cell. Group theory analysis, performed with the ISODISTORT software,[27] indicated four possible irreducible representations (irreps). Irreps mΓ^{1+} and mΓ^{3+} + mΓ^{4+} were not considered further as these gave rise to ferromagnetic ground states with moment along c and in the ab plane respectively. Irreps mΓ^{2-} and mΓ^{3-} $\oplus$ mΓ^{4-} gave rise to antiferromagnetic ground states, with spins aligned within the a,b plane for mΓ^{3-} $\oplus$ mΓ^{4-} and along the c axis for mΓ^{2-}. The mΓ^{3-} $\oplus$ mΓ^{4-} irrep is not consistent with the observed data, as this results in the 002 magnetic reflection at $d = 6.25$ Å being most intense magnetic reflection. This peak was not observed in the WISH data measured at 1.5 K. The mΓ^{2-} irrep was therefore refined against the 1.5 K dataset. The refinement profile for the data measured using the highest resolution back scattering bank ($2\theta = 152.8°$) is shown in Fig. 4a, and a representation of the magnetic structure is shown in Fig. 4b. The magnetic structure is the same as that reported recently for $KRuO_4$,[13] and it is described in the magnetic space group $I4_1'/a'$. The ordered magnetic moment was refined to be 0.46(18) μ_B which is similar to that seen for $KRuO_4$ (0.57 μ_B).[13] The small observed ordered moment is consistent with an enhanced spin–orbit coupling effect brought about by the more diffuse nature of the 5d orbitals, as well as the presence of short-range magnetic fluctuations, as is evidenced by bulk magnetic and heat capacity measurements. The absence of observable diffuse magnetic scattering features that would confirm the presence of short range correlations is presumably a result of the low magnetic scattering of the Os^{7+} cation.

The quantum magnetic material $KOsO_4$ has been synthesized, and determined to crystallise in the archetypal scheelite structure in space group $I4_1/a$. No structural phase transitions were observed between 1.5 K and decomposition up to 720 K. The material was found to possess long range anti-ferromagnetic order below 35 K, with the magnetic moments aligned along the c axis, with a magnitude of 0.46(18) μ_B per Os^{7+}. The small observed magnetic moment is likely brought about by diffuse

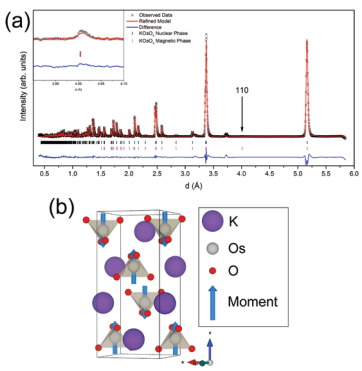

Fig. 4 (a) Rietveld refinement profile of NPD data collected at WISH at 1.5 K in the back-scattering detector bank with average 2θ of 152.8°. Observed data are indicated by black crosses, calculated profile is indicated by a red line and difference plot is shown in blue. Black tick marks indicate allowed *hkl* reflections of the nuclear phase, while magenta tick marks show allowed *hkl* positions of the magnetic phase. The 110 reflection of the magnetic phase is indicated, and shown in the inset. An unknown impurity is present and is responsible for the unfitted reflections evident near $d = 3.4$ and 3.7 Å. (b) Representation of the nuclear and magnetic structure of $KOsO_4$ at 1.5 K.

ordering, as is suggested by bulk magnetic and heat capacity measurements as well as a pronounced spin–orbit coupling effect, and electron delocalization due to the more diffuse nature of the 5d orbitals. The isolated nature of the OsO_4 tetrahedra, coupled with the lack of oxygen mediated super exchange results in weak direct interaction between the OsO_4 tetrahedra, leading to an antiferromagnetic ground state with evidence of short-range magnetic ordering, resulting in a reduced ordered magnetic moment. Overall this study represents the first case of a structural and magnetic characterization of a simple Os^{7+}, $S = 1/2$ oxide system, and provides a foundation for further investigation of related $AOsO_4$ and $ARuO_4$ compounds.

Conflicts of interest

There are no conflicts to declare.

Acknowledgements

We acknowledge the Australian Research Council for support of this work which was, in part, performed at the Powder Diffraction and X-ray Absorption Spectroscopy beamlines at the Australian Synchrotron and beamtime allocation from the Science and Technology Facilities Council, at the WISH at ISIS. We would like to thank Dr Paula Kayser Gonzalez for synthesis of the Os XAS standards, and Drs Helen Brand and Bernt Johannassen for their assistance at the powder diffraction and X-ray absorption spectroscopy beamlines at the Australian Synchrotron respectively.

Notes and references

1 H. L. Feng, S. Calder, M. P. Ghimire, Y.-H. Yuan, Y. Shirako, Y. Tsujimoto, Y. Matsushita, Z. Hu, C.-Y. Kuo, L. H. Tjeng, T.-W. Pi, Y.-L. Soo, J. He, M. Tanaka, Y. Katsuya, M. Richter and K. Yamaura, *Phys. Rev. B*, 2016, **94**, 235158.
2 A. S. Cavichini, M. T. Orlando, J. B. Depianti, J. L. Passamai Jr, F. Damay, F. Porcher and E. Granado, *Phys. Rev. B*, 2018, **97**, 054431.
3 Q. Chen, C. Svoboda, Q. Zheng, B. C. Sales, D. G. Mandrus, H. Zhou, J.-S. Zhou, D. McComb, M. Randeria and N. Trivedi, *Phys. Rev. B*, 2017, **96**, 144423.
4 J. P. Clancy, N. Chen, C. Y. Kim, W. F. Chen, K. W. Plumb, B. C. Jeon, T. W. Noh and Y.-J. Kim, *Phys. Rev. B: Condens. Matter Mater. Phys.*, 2012, **86**, 195131.
5 B. J. Kim, H. Jin, S. J. Moon, J. Y. Kim, B. G. Park, C. S. Leem, J. Yu, T. W. Noh, C. Kim, S. J. Oh, J. H. Park, V. Durairaj, G. Cao and E. Rotenberg, *Phys. Rev. Lett.*, 2008, **101**, 076402.
6 Y. Shi, Y. Guo, Y. Shirako, W. Yi, X. Wang, A. A. Belik, Y. Matsushita, H. L. Feng, Y. Tsujimoto and M. Arai, *J. Am. Chem. Soc.*, 2013, **135**, 16507–16516.
7 H. Shinaoka, T. Miyake and S. Ishibashi, *Phys. Rev. Lett.*, 2012, **108**, 247204.
8 A. S. Erickson, S. Misra, G. J. Miller, R. R. Gupta, Z. Schlesinger, W. A. Harrison, J. M. Kim and I. R. Fisher, *Phys. Rev. Lett.*, 2007, **99**, 016404.
9 K. W. Lee and W. E. Pickett, *Europhys. Lett.*, 2007, **80**, 37008.
10 C. A. Marjerrison, C. M. Thompson, G. Sala, D. D. Maharaj, E. Kermarrec, Y. Cai, A. M. Hallas, M. N. Wilson, T. J. S. Munsie, G. E. Granroth, R. Flacau, J. E. Greedan, B. D. Gaulin and G. M. Luke, *Inorg. Chem.*, 2016, **55**, 10701–10713.
11 K. E. Stitzer, M. D. Smith and H. C. zur Loye, *Solid State Sci.*, 2002, **4**, 311–316.
12 H. J. Xiang and M. H. Whangbo, *Phys. Rev. B: Condens. Matter Mater. Phys.*, 2007, **75**, 052407.
13 C. A. Marjerrison, C. Mauws, A. Z. Sharma, C. R. Wiebe, S. Derakhshan, C. Boyer, B. D. Gaulin and J. E. Greedan, *Inorg. Chem.*, 2016, **55**, 12897–12903.
14 W. Levason, M. Tajik and M. Webster, *J. Chem. Soc., Dalton Trans.*, 1985, 1735–1736, DOI: 10.1039/DT9850001735.
15 K. M. Mogare, W. Klein and M. Jansen, *Z. Anorg. Allg. Chem.*, 2005, **631**, 468–471.
16 S. Yonezawa, Y. Muraoka, Y. Matsushita and Z. Hiroi, *J. Phys.: Condens. Matter*, 2004, **16**, L9.
17 Y.-J. Song, K.-H. Ahn, K.-W. Lee and W. E. Pickett, *Phys. Rev. B: Condens. Matter Mater. Phys.*, 2014, **90**, 245117.
18 K. S. Wallwork, B. J. Kennedy and D. Wang, *AIP Conf. Proc.*, 2007, **879**, 879.
19 J. Rodriguez-Carvajal, *Physica B*, 1993, **192**, 55–69.
20 K.-D. Liss, B. Hunter, M. Hagen, T. Noakes and S. Kennedy, *Physica B*, 2006, **385–386**, 1010–1012.
21 L. C. Chapon, P. Manuel, P. G. Radaelli, C. Benson, L. Perrott, S. Ansell, N. J. Rhodes, D. Raspino, D. Duxbury and E. Spill, *J. Neutron Res.*, 2011, **22**, 22–25.
22 C. Glover, J. McKinlay, M. Clift, B. Barg, J. Boldeman, M. Ridgway, G. Foran, R. Garrett, P. Lay and A. Broadbent, *AIP Conf. Proc.*, 2007, **882**, 884–886.
23 B. Ravel and M. Newville, *J. Synchrotron Radiat.*, 2005, **12**, 537–541.
24 B. Krebs and K.-D. Hasse, *Acta Crystallogr., Sect. B: Struct. Crystallogr. Cryst. Chem.*, 1976, **32**, 1334–1337.
25 P. Kayser, S. Injac, B. J. Kennedy, T. Vogt, M. Avdeev, H. E. Maynard-Casely and Z. M. Zhang, *Inorg. Chem.*, 2017, **56**, 6565–6575.
26 R. S. Craig, S. G. Sankar, N. Marzouk, V. U. S. Rao, W. E. Wallace and E. Segal, *J. Phys. Chem. Solids*, 1972, **33**, 2267–2274.
27 B. J. Campbell, H. T. Stokes, D. E. Tanner and D. M. Hatch, *J. Appl. Crystallogr.*, 2006, **39**, 607–614.